



## Adsorption of sulfonamides from aqueous solution by carbon nanotubes: determination of kinetics, equilibrium and thermodynamic parameters

Chung-Hsin Wu\*, Shun-Chi Tsai

Department of Chemical and Materials Engineering, National Kaohsiung University of Science and Technology, 415 Chien Kung Road, Kaohsiung, Taiwan, Tel. 886-7-3814526; Fax: 886-7-3830674; emails: wuch@nkust.edu.tw (C.-H. Wu), j108246112@nkust.edu.tw (S.-C. Tsai)

Received 11 July 2021; Accepted 29 November 2021

### ABSTRACT

Adsorption by carbon nanotubes (CNTs) was used to remove sulfonamides (SAs) from aqueous solution. The target SAs were sulfamethoxazole (SMX) and sulfamethazine (SMZ). The effects of contact time, solution pH, CNTs dosage, initial SA concentration and temperature on the adsorption of SAs were determined. The pseudo-first-order, pseudo-second-order and intraparticle diffusion models were used to simulate the kinetics, and Langmuir and Freundlich's isotherms were employed to simulate the equilibrium. The adsorption of SAs onto CNTs best-fitted pseudo-second-order and Langmuir models. The adsorption amount of SAs increased with pH, CNTs dosage and temperature decreasing; conversely, it increased with initial SAs concentration increasing. The maximum adsorbed amounts of SMX and SMZ at pH 3 were 207.0 and 181.5 mg/g, respectively. The novel contributions of this study to the field are the evaluation of the hydrophobic and electrostatic interactions that are involved in the adsorption of SAs and the determination that the octanol-water partitioning coefficient ( $K_{ow}$ ) of SAs is important in adsorption; moreover, pH is also found to be important in hydrophobic and electrostatic interactions. The standard enthalpy change and standard entropy change of SMX were  $-19.7$  kJ/mol and  $23.7$  J/mol K, respectively; and those of SMZ were  $-5.0$  kJ/mol and  $72.9$  J/mol K, respectively. The adsorption of SMX and SMZ onto CNTs was a spontaneous physisorption process.

*Keywords:* Adsorption; Carbon nanotubes; Sulfonamides; Kinetics; Isotherm; Thermodynamics

### 1. Introduction

Sulfonamides (SAs) are a class of synthetic antibiotics that are extensively used in stockbreeding and for human treatment, mainly owing to their low-cost and broad-spectrum antibiotic properties. Zhu et al. [1] observed that SAs in water samples that were collected from feedlot wastewater pools and irrigation ditches in Shanghai City had total concentrations of 198–323  $\mu\text{g/L}$ . SAs in environmental water cause serious harm to not only the natural environment but also human health. Owing to the extensive use of sulfamethoxazole (SMX) and sulfamethazine

(SMZ), these compounds have been frequently observed in aquatic environments [2–4]. Schwab et al. [2] found that the concentration of SMX in drinking water can reach 8.5  $\mu\text{g/L}$ . SMX has been found at higher concentrations than other SAs and consequently categorized as a persistent antibiotic [5]. The influent concentrations of SMZ in a wastewater treatment plant (WTP) in Canada were found to be 45 ng/L [4], and those of SMZ in a WTP in Korea were 164 ng/L; the corresponding effluent concentration was 144 ng/L [3]. SMZ has attracted widespread interest because it has been detected in large areas of farm soil at concentrations

\* Corresponding author.

over 10 mg/kg [6]. Hence, SMX and SMZ were selected as the target SAs in this study.

A range of advanced wastewater treatment methods such as oxidation, catalytic degradation, adsorption, membrane filtration, ion exchange, solvent extraction, steam stripping, and microbial degradation have been developed for removing SAs from the environment. However, most of these consume considerable electricity and resources and may yield more toxic by-products [7,8], which need further treatment. Adsorption is an effective treatment technique for removing organic pollutants, such as pharmaceuticals and pesticides, from wastewater [9–11]. Limitations on the adsorption of various adsorbents must be specifically determined for each compound of interest.

Adsorption is a potential method for removing SAs; it is simple, stable, and highly efficient, and forms no or a small amount of toxic by-products. Carbon-based materials are widely used as highly effective adsorbents in removing contaminants from the aqueous solution because of their large specific surface area, high porosity, and high reaction activity [12]. The adsorptive removal of SAs with various carbon materials has been considered to be efficient [9–11,13,14]. Carbon nanotubes (CNTs) have favorable physicochemical and electrical characteristics, including a large surface area, small pores, high porosity, thermal and chemical stability, and useful functionality [15,16]; they also have many potential remediation applications, including the remediation of pharmaceutical chemicals such as SAs. The surface chemical functionalization of CNTs can improve their adsorption capacity by providing adsorption sites and functional groups. High-surface-area CNTs whose surfaces do not need to be modified and that adsorb large amounts of SMX and SMZ, are used herein. The adsorption of SMX and SMZ by CNTs was investigated using batch experiments. The objectives of this study

are (i) to evaluate the effects of contact time, solution pH, CNTs dosage, initial SA concentration and temperature on SAs adsorption; (ii) to investigate the adsorption of SMX and SMZ on CNTs with respect to adsorption kinetics and isotherms and (iii) to determine the thermodynamic parameters of adsorption.

## 2. Materials and methods

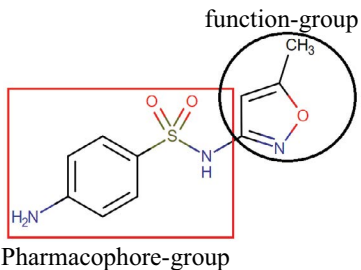
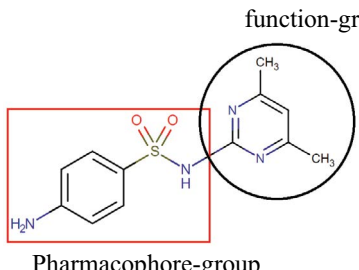
### 2.1. Materials

SMX and SMZ were purchased from Alfa Aesar (USA). Table 1 provides their physicochemical properties. Both SMX and SMZ have the same pharmacophore group. Sodium persulfate ( $\text{Na}_2\text{S}_2\text{O}_8$ ) and phosphoric acid ( $\text{H}_3\text{PO}_4$ ) were purchased from Sigma-Aldrich (USA). Multi-walled carbon nanotubes (MWCNTs) (purity > 98.5%) were purchased from Conjutek Materials Tech Co., Ltd., (Taiwan). MWCNTs were used as CNTs because they have wider range of applications than single-walled carbon nanotubes. The pH of the solution was controlled by adding  $\text{HNO}_3$  and  $\text{NaOH}$ , both of which were purchased from Merck (USA). All reagents were of analytical grade and used without further purification. Deionized water (DI) was used throughout this study.

### 2.2. Characterization of CNTs

The morphologies of the CNTs were obtained by scanning electron microscopy (SEM, JEOL 6330 TF, Japan) and transmission electron microscopy (TEM, JEOL 3010, Japan). The specific surface areas of the CNTs were calculated by the Brunauer–Emmett–Teller (BET) method, using nitrogen adsorption isotherms that were acquired at 77 K using an ASAP 2020 from Micromeritics Instrument Corporation (USA). The zeta potentials of CNTs that were suspended in

Table 1  
The physicochemical characteristics of SMX and SMZ

Compound name	SMX	SMZ
CAS no.	723-46-6	57-68-1
Molecular structure		
Molecular formula	$\text{C}_{10}\text{H}_{11}\text{N}_3\text{O}_3\text{S}$	$\text{C}_{12}\text{H}_{14}\text{N}_4\text{O}_2\text{S}$
Molecular weight	253.27 g/mol	278.33 g/mol
Solubility	610 mg/L <sup>a</sup>	1,500 mg/L <sup>b</sup>
$\log(K_{ow})$	0.85 <sup>a</sup>	0.14 <sup>b</sup>
Dissociation constants	$\text{pK}_{a1} = 1.80^a$ ; $\text{pK}_{a2} = 5.46^a$	$\text{pK}_{a1} = 2.65^b$ ; $\text{pK}_{a2} = 7.65^b$
References	<sup>a</sup> Wei et al. [17]; <sup>b</sup> Peiris et al. [18]	

$\log(K_{ow})$ : partition coefficient between water and octanol

DI water at various pH values were measured using a zeta potential analyzer (BIC 90 plus, USA), ten measurements were made at each pH and the average was obtained as the corresponding zeta potential.

### 2.3. Adsorption experiments

Kinetic studies were performed to determine the time required for the adsorption of SMX and SMZ onto CNTs to reach equilibrium. Equilibrium studies were conducted to determine the CNTs behavior, the amounts adsorbed at equilibrium, and the corresponding equilibrium constants. All experiments were conducted in an incubator shaker at 100 rpm. Kinetic adsorption experiments were performed with a CNTs dosage of 0.2 g/L and an initial SMX or SMZ concentration of 20 mg/L for 0–60 min at 308 K, and the total volume of the adsorption reaction system was 500 mL. A solution pH of 3 was maintained in all experiments, except in those for evaluating the effects of pH because this pH value yielded the most efficient sorption of SMX and SMZ. The various pH values of the suspension were achieved by adding 0.1 M HNO<sub>3</sub> or 0.1 M NaOH. In the experiments on the effect of pH ([SAs] = 20 mg/L and CNTs = 0.2 g/L), the pH of the solution was adjusted between 3 and 9. To investigate the effects of CNTs dosages, a series of dosages (0.1–0.3 g/L) were used with the same initial SAs concentration (20 mg/L); a series of SA concentrations (10–30 mg/L) were utilized at the same initial CNTs dose (0.2 g/L) to evaluate the effects of SA concentration.

To study the effects of temperature on the adsorption of SAs and to calculate the corresponding thermodynamic parameters, a batch experiment was conducted at the three temperatures of 308, 318 and 328 K for 24 h to ensure complete equilibrium. All samples were filtered through 0.45 μm polyvinylidene fluoride membrane filters (Whatman). The supernatant was removed and the residual CNTs were re-suspended by adding 1 L of pH 11 NaOH solution to initiate the desorption experiment. Each desorption experiment was performed at 308 K for 5 d to measure the concentrations of released SMX and SMZ, and the SMX and SMZ desorption ratio was calculated using a mass balance. The oxidant Na<sub>2</sub>S<sub>2</sub>O<sub>8</sub> and the acidifier H<sub>3</sub>PO<sub>4</sub> were placed in an O.I. 1010 total organic carbon (TOC, Aurora 1030W/1088 Model, USA) analyzer. The decrease in TOC therein yielded the degree of adsorption of SAs. All experiments were performed in duplicate, and mean values were reported.

## 3. Results and discussion

### 3.1. Surface characteristics of CNTs

Figs. 1a and b display the SEM and TEM images of CNTs. They reveal that the CNTs were cylindrical and that the external and internal diameters were 14 and 4 nm, respectively. Additionally, the distance between the walls of the CNTs was approximately 0.3 nm and the TEM analysis verified that the CNTs had hollow structures. The interstitial channels, external grooves, and partial coating of the external surfaces of CNTs by a nanometer-thick layer of carbon all contributed to overall adsorption. The surface area

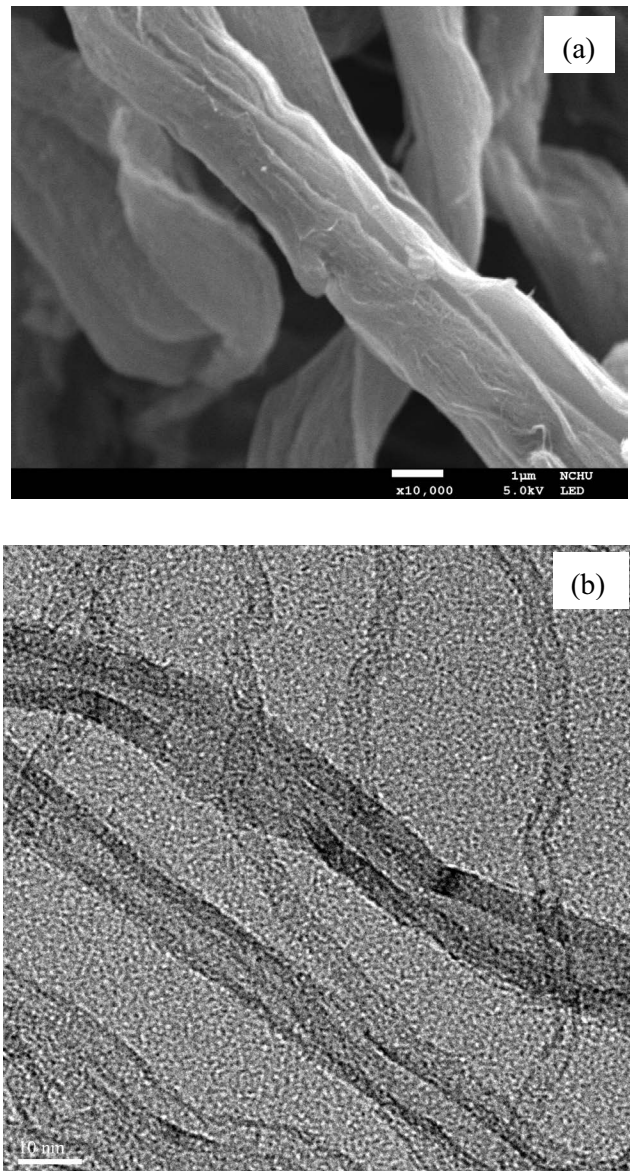


Fig. 1. Micrographs of CNTs (a) scanning electron microscopy and (b) transmission electron microscopy.

of the CNTs was determined to be 651 m<sup>2</sup>/g; the total pore volume was 1.54 cm<sup>3</sup>/g, and the zero point of charge of the CNTs was determined to be pH 4.8.

### 3.2. Kinetic studies

Kinetic models can reveal the migration behavior of SAs from the bulk solution to CNTs and describe the control mechanisms in the adsorption process. The kinetic equations, including pseudo-first-order, pseudo-second-order and intraparticle diffusion equations, were used in the simulation of the kinetics of adsorption. The pseudo-first-order model of Lagergren [19] assumes that the rate of adsorption of adsorbate is directly proportional to the difference in the saturation concentration [Eq. (1)]. The pseudo-second-order model of Ho and

McKay [20] assumes that the rate of adsorption depends on the amount of solute that is adsorbed at the adsorbent surface at time  $t$  and equilibrium [Eq. (2)]. The intraparticle diffusion model [21] assumes that the intraparticle diffusion is the rate-determining step of the adsorption process [Eq. (3)]. The term  $q_t$  (mg/g) represents the adsorption amount at time  $t$ ;  $q_e$  (mg/g) is the adsorption amount at equilibrium, and  $k_1$  ( $\text{min}^{-1}$ ) and  $k_2$  (g/mg min) are the pseudo-first-order and pseudo-second-order adsorption rate constants, respectively.  $k_i$  (mg/g  $\text{min}^{1/2}$ ) is the diffusion rate constant of intraparticle diffusion and  $C$  is the thickness of the boundary layer. Tables 2 and 3 present the simulated coefficients in the pseudo-second-order and intraparticle diffusion models, respectively.

$$\ln(q_e - q_t) = \ln q_e - k_1 t \quad (1)$$

$$\frac{t}{q_t} = \frac{1}{k_2 q_e^2} + \frac{t}{q_e} \quad (2)$$

$$q_t = k_i t^{1/2} + C \quad (3)$$

### 3.3. Effects of contact time and solution pH

Figs. 2a and b show the effects of pH on SMX and SMZ adsorption, respectively. After 10 min of adsorption, the SMX removal at pH 3, 5, 7 and 9 was 70%, 57%, 22% and

11% (Fig. 2a), respectively, and the SMZ removal was 70%, 69%, 56% and 26%, respectively (Fig. 2b). The removal rate was highest in the first 10 min. After this time, the adsorption gradually reached equilibrium and no effect of contact time on the amounts of SMX and SMZ adsorbed was detectable. The whole adsorption process could be divided into two stages – fast and slow. The fast adsorption stage was the first 10 min and was attributed mainly to the higher BET, abundant pore structure, the functional groups, and weak internal diffusion resistance [22]. The removal of SMX and SMZ then gradually approached equilibrium owing to the adsorption saturation effect. This initial fast step is attributable to the physical sorption of SAs onto CNTs by electrostatic forces upon initial contact. In contrast, the subsequent slow step may be related to chemical interactions between SAs and CNTs over long-term adsorption [23].

The fitting degree ( $R^2$ ) of the pseudo-second-order model exceeded that of the pseudo-first-order model. The adsorption amount that was calculated using the pseudo-second-order model ( $q_{e,cal}$ ) was consistent with that obtained experimentally ( $q_{e,exp}$ ) (Table 2). Since the pseudo-first-order model did not correlate closely with the experimental data points, the kinetic parameters that were determined from this model are not provided. The pseudo-second-order model includes three stages of adsorption – liquid film diffusion, intraparticle diffusion and surface adsorption – and it better fits the experimental adsorption process [24]. The result herein was consistent with that in previous investigations of the removal of organic matter by

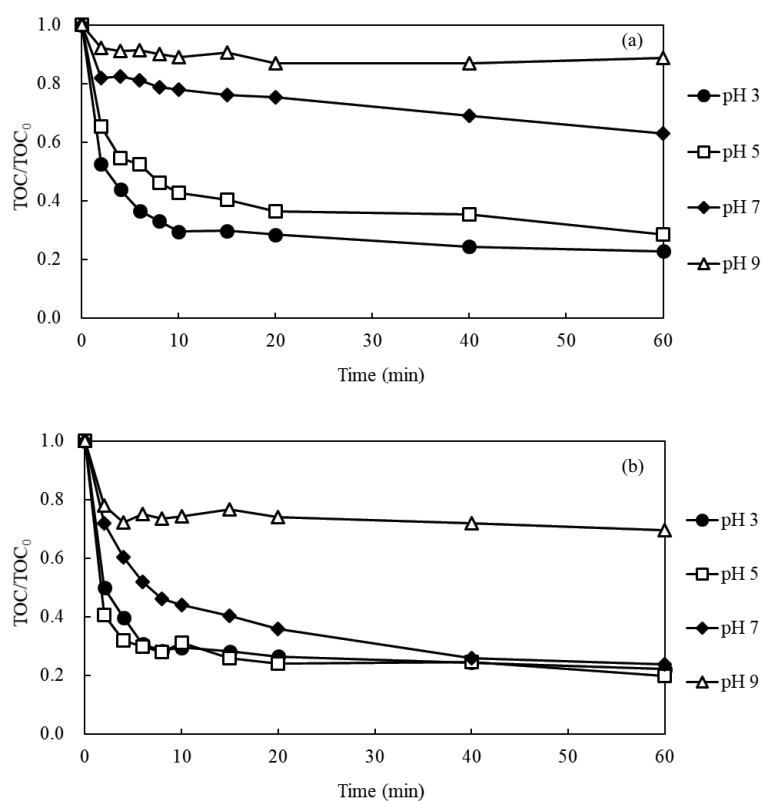


Fig. 2. Effects of pH on SAs adsorption (a) SMX and (b) SMZ ([SAs] = 20 mg/L; [CNTs] = 0.2 g/L;  $T = 308$  K).

Table 2  
Kinetic parameters of pseudo-second-order model

Pseudo-second-order model				
	$q_{e,exp}$ (mg/g)	$k_2$ (g/mg min)	$q_{e,cal}$ (mg/g)	$R^2$
SMX				
pH 3	81.0	0.0096	82.1	0.9992
pH 5	69.3	0.0061	69.8	0.9954
pH 7	35.1	0.0052	35.5	0.9676
pH 9	10.7	0.0850	11.4	0.9852
SMZ				
pH 3	72.1	0.0144	72.6	0.9994
pH 5	73.8	0.0153	73.5	0.9986
pH 7	73.2	0.0037	76.7	0.9945
pH 9	28.6	0.0227	28.3	0.9928
SMX				
0.3 g/L	56.8	0.0286	57.0	0.9996
0.2 g/L	81.0	0.0096	82.1	0.9992
0.1 g/L	97.9	0.0058	98.5	0.9971
SMZ				
0.3 g/L	55.6	0.0285	55.3	0.9988
0.2 g/L	72.1	0.0144	72.6	0.9994
0.1 g/L	89.9	0.0091	91.2	0.9985
SMX				
30 mg/L	106.6	0.0053	108.1	0.9984
20 mg/L	81.0	0.0096	82.1	0.9992
10 mg/L	40.3	0.0421	40.4	0.9997
SMZ				
30 mg/L	111.5	0.0047	110.0	0.9925
20 mg/L	72.1	0.0144	72.6	0.9994
10 mg/L	40.4	0.0346	40.5	0.9992

carbon-based materials, which were also found to obey the pseudo-second-order model [13,14,25,26].

A variation in pH not only affects the protonation-deprotonation transition of functional groups on CNTs, but also changes chemical speciation for ionizable SAs [27]. Ionizable SAs can interact with adsorbents through electrostatic attraction or repulsion, depending on their acidity constants ( $pK_a$ ). Cationic ( $SAs^+$ ), neutral ( $SAs^0$ ), and anionic ( $SAs^-$ ) compounds were formed as determined by two acid dissociation constants within a wide pH range. The first constant involves the protonation of the aniline N ( $pK_{a1}$ ) and the other entails deprotonation of the  $SAs'$  NH ( $pK_{a2}$ ). As the pH increased from 3 to 9, the  $SAs^+$  gradually transformed into  $SAs^0$  and then  $SAs^-$ . Sorption was maximal with the adsorption of neutral species ( $SAs^0$ ) of SAs [13]. The deprotonated anionic form is manifestly more hydrophilic than the protonated form, explaining the significantly stronger sorption of the protonated species than the anionic species. The effect of pH involved electrostatic and hydrophobic interactions. Hence, the adsorption

affinity of CNTs for various SAs species followed the order  $SAs^0 > SAs^+ > SAs^-$ . The SMX adsorption amounts at pH 3, pH 5, pH 7 and pH 9 were 81.0, 69.3, 35.1 and 10.7 mg/g, respectively, and those of SMZ were 72.1, 73.8, 73.2 and 28.6 mg/g, respectively (Table 2). The ratio of SMX<sup>0</sup> in solution at pH 3, pH 5, pH 7 and pH 9 was 0.938, 0.742, 0.028 and 0, respectively; hence, the adsorption amounts of SMX followed the order pH 3 > pH 5 > pH 7 > pH 9. The ratios of SMZ<sup>0</sup> in solution at pH 3, pH 5, pH 7 and pH 9 were 0.691, 0.993, 0.817 and 0.043, respectively; accordingly, the adsorption amounts of SMZ followed the order pH 5 > pH 7 > pH 3 > pH 9. The adsorption of SMX at different pH values onto CNTs was also examined by Jakubus et al. [28] and Liu et al. [25], who found that the adsorption of SMX was greatest when the solution was adjusted to pH 3; this finding was consistent with the results in this work.

Electrostatic interaction is responsible for the lower adsorption amounts at higher pH values. The isoelectric point of CNTs was determined to be pH 4.8. The CNTs were negatively charged at pH values of higher than 4.8; otherwise, the surface of CNTs was positively charged by protonation. Due to the electrostatic repulsion between  $SAs^-$  and negatively charged CNTs, the adsorption capacity was lower at higher pH. The decrease in the adsorption by CNTs was attributed to an increase in ionization with pH, which reduces the hydrophobic interaction [29] and strengthens the electrostatic repulsion between SAs and CNTs. Hence, the amounts of both SMX and SMZ that were adsorbed were lowest at pH 9.

Diffusion models are important for identifying the diffusion mechanisms and rate-controlling steps of adsorption. The whole adsorption process has three stages: (1) stage I is liquid film diffusion (in which adsorbate is transported from the bulk solution to the external surface of the adsorbent, in a process that is also called outer diffusion); (2) stage II is intraparticle diffusion (in which adsorbate from the exterior of the adsorbents enters internal pores); and (3) stage III is the adsorptive attachment equilibrium stage (in which adsorbate binds to the active sites of the outer surfaces or interior of adsorbents. However, stage III is not regarded as the rate-limiting step because of its high speed [22]. The kinetic data were fitted using the intraparticle diffusion model (Table 3). The multi-linear curves revealed that the whole adsorption process is controlled by a multistep mechanism, including boundary layer diffusion and intraparticle diffusion, and the fall in rate constants with time is attributable to gradual saturation of the adsorbent surface [30]. The regression of the intraparticle diffusion model did not pass through the origin and exhibited multilinearity, suggesting that the adsorption involved several diffusion processes. Additionally, stage I (liquid film diffusion) and stage II (intraparticle diffusion) simultaneously controlled the adsorption rate [31]. Since no C value was zero (Table 3), surface adsorption and intraparticle diffusion simultaneously occurred during the interaction between SAs and CNTs.

#### 3.4. Effects of CNTs dosage and initial SAs concentration

After 10 min of adsorption, SMX removal at CNTs doses of 0.1, 0.2 and 0.3 g/L was 48%, 70% and 83%, respectively,

Table 3  
Kinetic parameters of intraparticle diffusion model

	Intraparticle diffusion model		
	$k_i$ (mg/g min <sup>1/2</sup> )	C (mg/g)	$R^2$
SMX			
pH 3	8.04	43.6	0.8152
pH 5	8.73	24.9	0.9303
pH 7	2.42	12.7	0.9168
pH 9	1.36	5.4	0.7373
SMZ			
pH 3	6.31	43.5	0.7143
pH 5	4.17	52.2	0.7917
pH 7	10.82	16.8	0.9120
pH 9	0.23	22.9	0.0181
SMX			
0.3 g/L	3.83	40.0	0.6886
0.2 g/L	8.04	43.6	0.8152
0.1 g/L	10.38	44.3	0.8943
SMZ			
0.3 g/L	4.20	37.4	0.8198
0.2 g/L	6.31	43.5	0.7143
0.1 g/L	14.07	33.9	0.8983
SMX			
30 mg/L	11.15	51.0	0.9030
20 mg/L	8.04	43.6	0.8152
10 mg/L	1.93	30.8	0.9216
SMZ			
30 mg/L	6.98	65.1	0.9132
20 mg/L	6.31	43.5	0.7143
10 mg/L	4.41	22.7	0.5964

and SMZ removal was 46%, 70% and 85%, respectively (figure not showed here). An increase in CNTs dosage and contact time increased adsorption owing to the availability of a larger surface area of the CNTs with many active sites where SAs can attach during the adsorption process. The adsorption amounts of SMX at CNTs doses of 0.1, 0.2 and 0.3 g/L were 97.9, 81.0 and 56.8 mg/g, respectively, and those of SMZ were 89.9, 72.1 and 55.6 mg/g, respectively (Table 2). A larger CNTs dosage resulted in a lower adsorption amount for SAs. The decline in the trend was due to the agglomeration of a higher dose of CNTs, hence, the CNTs adsorptive amount cannot be fully utilized at a higher CNTs dosage in comparison to lower CNTs dosage. A higher dose of CNTs provided more active sites for SA adsorption. The adsorption rate is governed by adsorption at active sites. The value of  $k_2$  increased with CNTs dosage (Table 2), as a result of a strengthening of the driving force of diffusion.

After 10 min of adsorption, SMX removal at initial SMX concentrations of 10, 20 and 30 mg/L was 72%, 70% and 61%, respectively, and that of SMZ was 77%, 70% and

65%, respectively (figure not shown here). Increasing the initial SMX concentration from 10 up to 30 mg/L increased the adsorption amount from 40.3 to 106.6 mg/g; for SMZ, the corresponding increase is from 40.4 to 111.5 mg/g (Table 2). The adsorption amount increased with the initial concentration of SAs while the removal efficiency of SAs decreased. SAs molecules tended to diffuse more toward active adsorption sites of CNTs at higher SAs concentrations, resulting in greater adsorption. The decrease in the adsorption percentage arose from the saturation of the active sites of the CNTs, inhibiting the attachment of more molecules of SAs. An insufficient number of active sites on CNTs reduced the efficiency of removal by CNTs at high SAs concentration. Therefore, the decrease of  $k_2$  with increasing initial concentration of SAs is attributable to the availability of active sites on the surface of CNTs (Table 2).

The intercept [Eq. (3)],  $C$ , provides information on the thickness of the boundary layer. The resistance to external mass transfer increases as the intercept increases [32]. The constant  $C$  increases from 30.8 to 51.0 mg/g as the SMX concentration increases from 10 to 30 mg/L, respectively; and from 22.7 to 65.1 mg/g as the SMZ concentration increases from 10 to 30 mg/L, respectively (Table 3). These results show an increase in the thickness of the boundary layer and a decrease in the probability of external mass transfer. The  $C$  value increased with initial SAs concentration, indicating that boundary layer diffusion was stronger at higher SAs concentration [33].

### 3.5. Effects of compound's properties

The octanol-water partitioning coefficient ( $K_{ow}$ ) and  $pK_a$  were important in assessing the adsorption behaviors of different SAs.  $K_{ow}$  is commonly used as an index of an adsorbate's hydrophobicity and  $pK_a$  is related to the speciation of SAs [26]. The much higher hydrophobicity of SAs<sup>0</sup> species than of SAs<sup>+</sup> and SAs<sup>-</sup> species is mainly responsible for its greater adsorption affinity [34]. The hydrophobicity of pollutants can reportedly affect their adsorption, and the relationship is positive for a hydrophobic pollutant, as revealed by  $K_{ow}$  [35]. Zhao et al. [36] observed that the order of hydrophobic for the heterocyclic amines was consistent with adsorption affinities of the SAs, which indicated that the adsorption difference of SAs was affected by the hydrophobic of different substituents. A larger  $\log K_{ow}$  corresponds to greater hydrophobicity, so SMX ( $\log K_{ow} = 0.85$ ) underwent more hydrophobic adsorption than SMZ ( $\log K_{ow} = 0.14$ ). More SMX (81.0 mg/g) than SMZ (72.1 mg/g) was adsorbed onto CNTs at pH 3 (Table 2) owing to its relatively high hydrophobicity (Table 1). The hydrophobic attraction between the SAs and CNTs was the dominant adsorption mechanism at pH 3 herein. Additionally, the adsorption amounts of the SAs were mainly affected by electrostatic attraction at pH 5–9, and the hydrophobic effect contributed only weakly to the removal of both SMX and SMZ by adsorption onto CNTs. Less SMX than SMZ was adsorbed onto CNTs at pH 5–9 (Table 2). Gao et al. [37] found that the main adsorption mechanisms between activated carbon (AC) and fluoroquinolone antibiotics were a hydrophobic attraction and electrostatic interaction. Deng et al. [38] investigated the

adsorption of six perfluorinated compounds and found that hydrophobic interactions and electrostatic forces were responsible for their adsorption onto CNTs. The adsorption of SMX and SMZ under the same conditions was governed by a combination of forces. Liu et al. [25] suggested that the adsorption of SAs onto CNTs at pH 3 is mainly governed by an electron-donor-acceptor interaction and a non-hydrophobic interaction. The biosorption efficiencies of extracellular polymeric substances (EPS) were 70% and 53% for SMX and SMZ, respectively [23]. Pi et al. [23] suggested that the higher adsorption efficiency for SMX than SMZ on EPS at pH 4 might be attributed to the weaker steric hindrance of the function group, easily occupying more adsorption sites. The higher adsorption efficiency for SMX than SMZ onto CNTs was as identified by Pi et al. [23]. The findings in this study suggest that the hydrophobic interaction and electrostatic interaction were involved in the adsorption of SAs by CNTs and pH importantly affected the balance between hydrophobic and electrostatic interactions.

3.6. Adsorption isotherms

Equilibrium data for the adsorption of SMX and SMZ onto CNTs were analyzed using the Langmuir [39] and Freundlich [40] models. The adsorption isotherms are as described below. The Langmuir model [Eq. (4)] describes the monolayer adsorption of a compound onto a surface with a finite number of identical sites without surface diffusion. The Freundlich model [Eq. (5)] assumes multilayer adsorption,

and describes physisorption on a heterogeneous surface with various binding sites [41].

$$q_e = \frac{q_m K_L C_e}{(1 + K_L C_e)} \tag{4}$$

$$q_e = K_f C_e^{\frac{1}{n}} \tag{5}$$

$$R_L = \frac{1}{1 + K_L C_0} \tag{6}$$

where  $C_e$  is the concentration of TOC at equilibrium;  $C_0$  is the concentration of TOC at  $t = 0$ ;  $K_L$  is the Langmuir adsorption constant; and  $q_m$  (mg/g) is the theoretical maximum adsorption amount.  $R_L$  is the separation factor [Eq. (6)], which specifies whether the adsorption process is unfavorable ( $R_L > 1$ ), linear ( $R_L = 1$ ), favorable ( $0 < R_L < 1$ ), or irreversible ( $R_L = 0$ ),  $K_f$  and  $n$  are the Freundlich constants, and denote the adsorption capacity and process intensity;  $1/n$  indicates the type of isotherm:  $1/n \leq 0$ ,  $1/n > 1$ , and  $0 < 1/n < 1$  indicate irreversible, undesirable and desirable, respectively [9].  $R$  (8.314 J/mol K) is the gas constant.

Figs. 3 and 4 plot the adsorption isotherms of SMX and SMZ at various temperatures, respectively. The amounts of SMX and SMZ that were adsorbed onto CNTs increased with the temperature declined, indicating that reducing the temperature favored SMX and SMZ adsorption. A high temperature disfavored the adsorption reaction, so adsorption

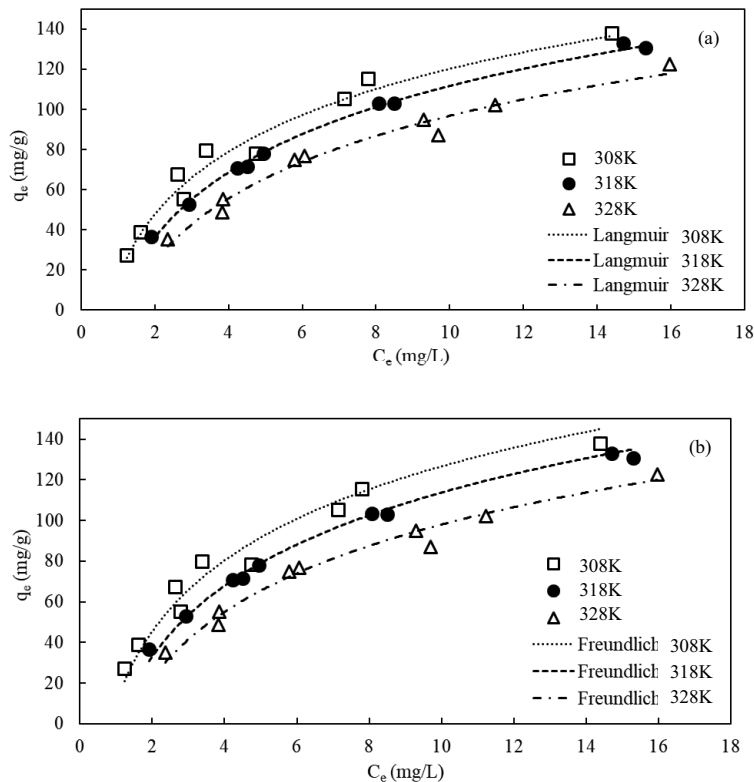


Fig. 3. Adsorption isotherm analyses of SMX (a) Langmuir and (b) Freundlich plots (pH = 3; contact time = 24 h).

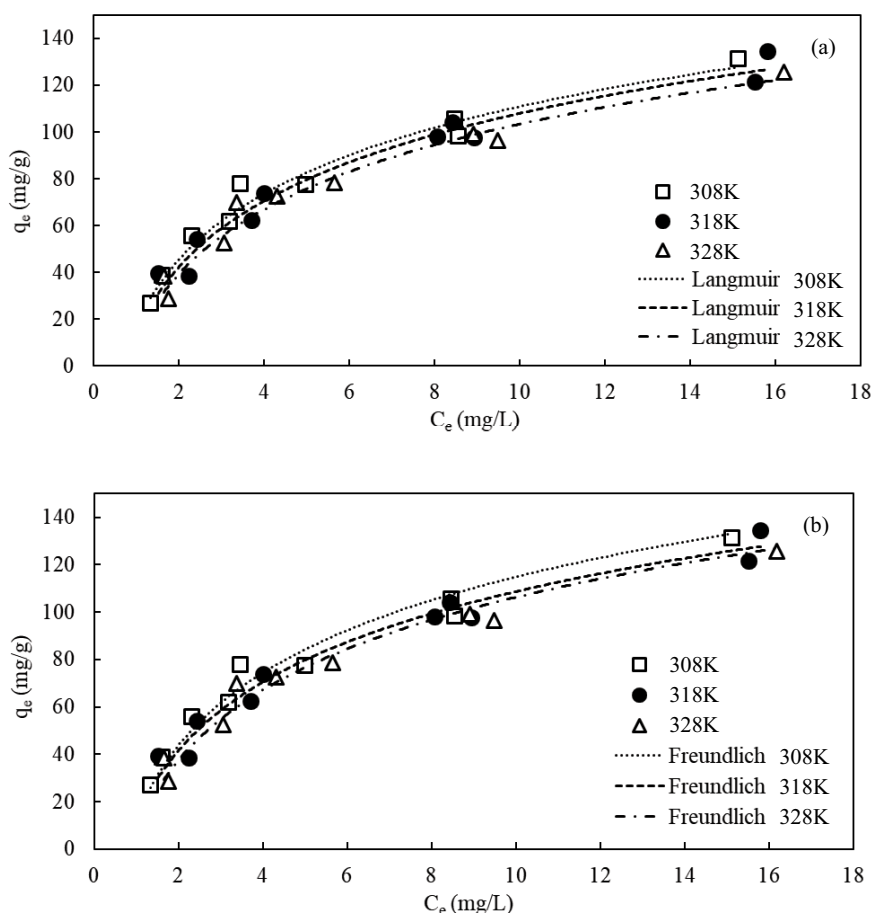


Fig. 4. Adsorption isotherm analyses of SMZ (a) Langmuir plots and (b) Freundlich plots (pH = 3; contact time = 24 h).

by CNTs was exothermic. The experimentally obtained equilibrium adsorption data were fitted using Langmuir and Freundlich isotherms. Both Langmuir and Freundlich isotherms fitted the experimental results ( $R^2 > 0.94$ ); moreover, the  $R^2$  of the Langmuir model exceeded that of the Freundlich model at the same temperature (Table 4). Tang et al. [42] and Pi et al. [23] found that the pseudo-second-order, Langmuir and Freundlich's models fitted the experimental data, revealing that both physisorption and chemisorption had participated critically in the SMX adsorption. The Langmuir and Freundlich isotherms both described the experimental data, indicating that SMX was adsorbed on the heterogeneous surface through multilayer and monolayer adsorption [43]. The results concerning the adsorption SMX and SMZ onto CNTs herein were similar to those of Tang et al. [42], Zheng et al. [43] and Pi et al. [23].

The essential feature of the Langmuir isotherm can be expressed using ' $R_L$ ', which is a dimensionless constant that is referred to as the "separation factor" or "equilibrium parameter". All values of  $R_L$  between 0 and 1 indicate that the adsorption of SMX and SMZ onto CNTs was favorable. For both SMX and SMZ, the maximum adsorption amount ( $q_m$ ) increased as temperature decreased, and the value for SMX exceeded that for SMZ at pH 3 at all tested temperatures (Table 4).

Table 5 compares the maximum adsorption amounts of SMX and SMZ onto various carbon-based materials. The maximum adsorption amounts of SMX and SMZ onto hexadecyltrimethylammonium bromide-modified AC according to the Langmuir model were 16.2 and 17.5 mg/g [14], respectively; the corresponding values onto functionalized biochar were 88.1 and 65.7 mg/g [13], respectively; and those onto AC were 231.7 and 206.6 mg/g [11], respectively. The maximum adsorption amount of SMX onto CNTs/CoFe<sub>2</sub>O<sub>4</sub> was 7.0 mg/g [47] and that of SMZ onto hydroxylated-CNTs was 21 mg/g [50]. The observed maximum adsorption amounts of SMX and SMZ onto CNTs herein exceeded those reported in other studies using various carbon-based materials.

The surface area that was covered by adsorbed SAs was obtained using Eq. (7) [11].

$$S_{\text{covered}} (\text{m}^2/\text{g}) = q_i \cdot N_A \cdot A_i \quad (7)$$

where  $S_{\text{covered}}$  is the surface area that was occupied by SAs in  $\text{m}^2/\text{g}$ ;  $q_i$  is the amount of adsorbed SA<sub>*i*</sub> in mol/g;  $N_A$  is the Avogadro number in molecules/mol;  $A_i$  is the projected area of SA<sub>*i*</sub> in  $\text{nm}^2/\text{molecule}$ . The value of  $A_i$  was 0.7221  $\text{nm}^2/\text{molecule}$  for SMX and 0.6919  $\text{nm}^2/\text{molecule}$  for SMZ [11];

Table 4  
Isotherm parameters for the SMX and SMZ adsorption onto CNTs (pH = 3)

Langmuir isotherm				
	$q_m$ (mg/g)	$K_L$ (L/mg)	$R^2$	$R_L$
SMX				
308 K	207.0	0.145	0.9925	0.263
318 K	206.5	0.119	0.9956	0.309
328 K	203.4	0.091	0.9942	0.375
SMZ				
308 K	181.5	0.162	0.9963	0.245
318 K	178.7	0.156	0.9980	0.256
328 K	177.0	0.144	0.9967	0.270
Freundlich isotherm				
	$n$	$K_f$	$R^2$	
SMX				
308 K	1.563	29.511	0.9446	
318 K	1.683	28.174	0.9671	
328 K	1.568	22.065	0.9687	
SMZ				
308 K	1.698	29.622	0.9587	
318 K	1.879	31.097	0.9725	
328 K	1.714	27.374	0.9606	

the values of  $q_i$  at 308K and pH = 3 were 0.817 mmol/g for SMX and 0.652 mmol/g for SMZ herein. Accordingly, substituting  $q_i$ ,  $N_A$  and  $A_i$  into Eq. (7) yielded total covered areas of 355.2 and 271.6 m<sup>2</sup>/g for SMX and SMZ adsorption, respectively, and which were 0.546 and 0.417 times the surface area of CNTs (651 m<sup>2</sup>/g), respectively. This study suggests that not all of the adsorption sites on CNTs were active for SMX and SMZ under the experimental conditions.

### 3.7. Distribution coefficient from equilibrium experiments and $K_{ow}$

A linear isotherm is obtained when the constant  $1/n$  in the Freundlich model is approximately unity. The linear isotherm closely describes the partition of a compound at low mass loading or when no specific bonding exists between the adsorbate and the adsorbent [Eq. (8)] [52]:

$$q_e = K_d \cdot C_e \quad (8)$$

where  $K_d$  is the distribution coefficient and  $q_e$  and  $C_e$  are as previously defined. Hence,  $K_d$  also defines the ratio of concentration in the aqueous phase to that in the solid phase.

In wastewater treatment, SAs are partitioned into the solid phase, depending on the hydrophobicity of compounds, which is related to the  $K_{ow}$  value. A larger  $K_{ow}$  indicates that the compound is more hydrophobic. Dobbs et al. [53] found that the adsorption of certain chlorinated organic compounds on primary and digested solids from

municipal WTPs correlated positively with their  $\log(K_{ow})$  values. Xia et al. [54] suggested that the  $K_d$  values of pharmaceutical compounds could be predicted from their  $K_{ow}$  values using the equation  $\log K_{d, \text{predicted}} = 0.58 \cdot \log K_{ow} + 1.14$ . The  $K_{d, \text{predicted}}$  values for SMX and SMZ were calculated as 43.0 and 16.4, respectively, in contrast to the experimentally determined (pH 3 and 308 K)  $K_d$  values of 8.0 and 6.9, respectively. Apparently, the  $K_{d, \text{predicted}}$  values were inconsistent with the  $K_d$  values; however, the trends of  $K_{d, \text{predicted}}$  and  $K_d$  values for SMX and SMZ were consistent.  $K_d$  did not completely dependent on  $K_{ow}$ , indicating that the hydrophobic property did not dominate the adsorption of SAs. Sun et al. [55] found that van der Waals forces and hydrophobicity played major roles in the adsorption of SAs onto biochar. Peng et al. [56] found that the major difference between the hydrophobicity of ofloxacin (OFL) and that of norfloxacin (NOR) did not result in a difference in their adsorption on CNTs. The similar structures of OFL and NOR cause the adsorption of both onto CNTs to be structurally controlled.

### 3.8. Thermodynamics analyses

The thermodynamic parameters of standard Gibbs free energy change ( $\Delta G^\circ$ ), standard enthalpy change ( $\Delta H^\circ$ ), and standard entropy change ( $\Delta S^\circ$ ) provide information on the energetic changes inherent to the adsorption process. The Langmuir isotherm was used to calculate thermodynamic parameters using Eqs. (9) and (10).  $\Delta H^\circ$  and  $\Delta S^\circ$  were determined from the slope and intercept of the van't Hoff plots of  $\ln(K_L)$  vs.  $1/T$  [Eq. (10)] [57].

$$\Delta G^\circ = -RT \ln(K_L) \quad (9)$$

$$\ln(K_L) = \frac{\Delta S^\circ}{R} - \frac{\Delta H^\circ}{RT} \quad (10)$$

Fig. 5 plots the regression of the van't Hoff equation. Table 6 presents the thermodynamic parameters of CNTs at various temperatures. The negative  $\Delta G^\circ$  values suggested that the adsorption of SMX and SMZ onto CNTs is spontaneous. The negative values of  $\Delta H^\circ$  reveal that the adsorption is exothermic. The positive  $\Delta S^\circ$  values suggest increasing randomness and disorder of the system during the adsorption process [43]. The adsorption of SMX onto CNTs released more energy (more negative  $\Delta H^\circ$  values) and exhibited greater orderliness (smaller  $\Delta S^\circ$  values) than that of SMZ. Both SMX and SMZ exhibited similar thermodynamic parameters, with their adsorption being spontaneous, exothermic, and entropically favorable. Pi et al. [23] also found that the adsorption of SMX and SMZ onto EPS decreased as the temperature increased.

The change in free energy ( $\Delta G^\circ$ ) for physisorption is reportedly in the range from 0 to -20 kJ/mol, while that in chemisorption is between -80 and -400 kJ/mol [58]. In this study, the  $\Delta G^\circ$  values were in the range from -26.9 to -28.9 kJ/mol (Table 6), indicating that adsorption proceeded mainly physisorption. Jaria et al. [10] suggested that the physisorption is always an exothermic process. Physisorption is characterized by a reduction in free energy and entropy, and therefore this form of adsorption

Table 5  
Comparisons of SMX and SMZ maximum adsorption amount onto various carbon-based materials

SAs	Adsorbent	$q_m$ (mg/g)	References
SMX	CNTs	206.5	This study
	Graphene	239.0	Chen et al. [44]
	AC	231.7	Serna-Carrizales et al. [11]
	Magnetic AC composites	159	Wan et al. [45]
	Biochar	99.1	Choi and Kan [46]
	Functionalized biochar	88.1	Ahmed et al. [13]
	Modified AC	16.2	Liu et al. [14]
	CNT/CoFe <sub>2</sub> O <sub>4</sub>	7.0	Wang et al. [47]
SMZ	CNTs	178.7	This study
	AC	206.6	Serna-Carrizales et al. [11]
	Graphene	104.9	Peng et al. [48]
	Functionalized biochar	65.7	Ahmed et al. [13]
	Biochar	33.8	Rajapaksha et al. [49]
	Hydroxylated-CNTs	21.0	Yang et al. [50]
	Modified AC	17.5	Liu et al. [14]
	Modified AC	17.2	Liu et al. [51]

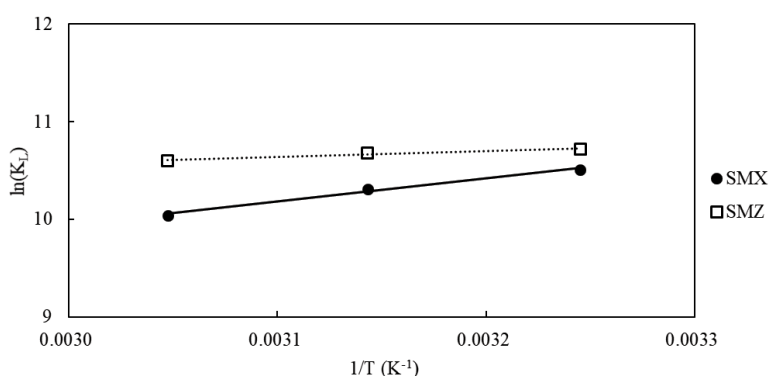


Fig. 5. Regressions of van't Hoff plot for thermodynamic parameters.

is exothermic, so it happens quite rapidly at low temperatures and becomes significantly weaker as the temperature increases [59]. The negative value of  $\Delta H^\circ$  herein confirmed that the adsorption of SAs was exothermic. Alkan et al. [60] and Zhao et al. [61] suggested that the adsorption is governed by chemisorption when the value of  $\Delta H^\circ$  is between 40 and 120 kJ/mol. Kara et al. [62] suggested that a heat of adsorption of less than 40 kJ/mol implies physisorption. Moreover, the heat that is evolved in physisorption is of the same order of magnitude as the heat of condensation, 2.1–20.9 kJ/mol [63]. In this investigation, the  $\Delta H^\circ$  values of SMX and SMZ were  $-19.7$  and  $-5.0$  kJ/mol (Table 6), respectively, showing that the adsorption of SMX and SMZ onto CNTs is a physisorption process.

### 3.9. Desorption

Fig. 6 plots the desorption of SMX and SMZ over time. The aqueous concentrations of SAs increased rapidly during the first day of desorption, approaching steady values, which are held constant for the following

Table 6  
Thermodynamic parameters of CNTs at various temperatures

	$\Delta G^\circ$ (kJ/mol)	$\Delta H^\circ$ (kJ/mol)	$\Delta S^\circ$ (J/mol K)
SMX			
308 K	$-26.9$	$-19.7$	23.7
318 K	$-27.3$		
328 K	$-27.4$		
SMZ			
308 K	$-27.5$	$-5.0$	72.9
318 K	$-28.2$		
328 K	$-28.9$		

4 d. As shown in Fig. 6, many more SMX molecules (81%) than the SMZ molecules (46%) were desorbed. At pH 11, the electrostatic attraction of SAs is mainly responsible for their adsorption; hence, the desorption percentage of SMZ

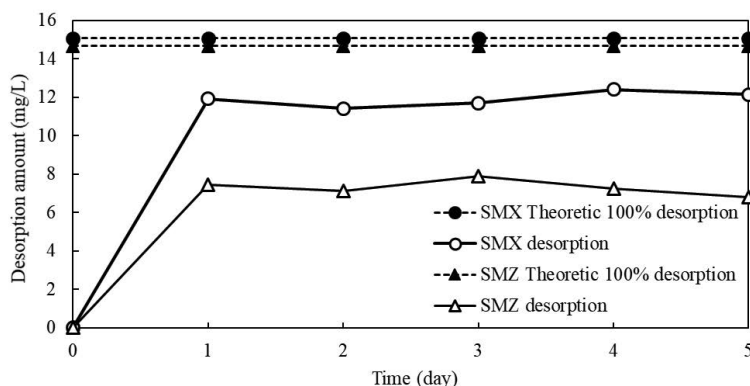


Fig. 6. Desorption of SMX and SMZ from the used CNTs (pH = 11; T = 308 K).

onto CNTs was lower than that of SMX because the electrostatic attraction was stronger. The physisorption was caused by the reversible weak intermolecular physical interactions, such as diffusion, hydrophobic interactions, electrostatic attraction and hydrogen bonding with the multilayer formation of adsorbate on the adsorbent. The results concerning desorption again suggest that the adsorption of SMX and SMZ onto CNTs involved physisorption.

#### 4. Conclusions

The solution pH was an important parameter in the adsorption of SAs onto CNTs, owing to its effects on the chemical speciation of SAs and the surface electrical property of CNTs. The hydrophobic attraction between the SAs and CNTs was the dominant adsorption mechanism at pH 3, whereas the amount of SAs adsorbed was dominated by electrostatic attraction at pH 5–9. The Langmuir model best fitted the SMX and SMZ adsorption onto CNTs, indicating the formation of a monolayer. Not all adsorption sites on CNTs were active for SMX and SMZ under the experimental conditions herein. The negative  $\Delta G^\circ$  and  $\Delta H^\circ$  and positive  $\Delta S^\circ$  values indicated the spontaneous and exothermic nature of the adsorption process, which is accompanied by an increase in entropy and governed by a physisorption mechanism.

#### Acknowledgments

The authors would like to thank the Ministry of Science and Technology for financially supporting this research under Contract No. 109-2221-E-992-050.

#### References

- [1] L. Zhu, H. Xu, W. Xiao, J. Lu, D. Lu, X. Chen, X. Zheng, E. Jeppesen, W. Zhang, L. Wang, Ecotoxicological effects of sulfonamide on and its removal by the submerged plant *Vallisneria natans* (Lour.) Hara, *Water Res.*, 170 (2020) 115354, doi: 10.1016/j.watres.2019.115354.
- [2] B.W. Schwab, E.P. Hayes, J.M. Fiori, F.J. Mastrocco, N.M. Roden, D. Cragin, R.D. Meyerhoff, V.J. D'Aco, P.D. Anderson, Human pharmaceuticals in US surface waters: a human health risk assessment, *Regul. Toxicol. Pharm.*, 42 (2005) 296–312.
- [3] S.K. Behera, H.W. Kim, J.-E. Oh, H.-S. Park, Occurrence and removal of antibiotics, hormones and several other pharmaceuticals in wastewater treatment plants of the largest industrial city of Korea, *Sci. Total Environ.*, 409 (2011) 4351–4360.
- [4] P. Guerra, M. Kim, A. Shah, M. Alaei, S.A. Smyth, Occurrence and fate of antibiotic, analgesic/anti-inflammatory, and antifungal compounds in five wastewater treatment processes, *Sci. Total Environ.*, 473–474 (2014) 235–243.
- [5] D.W. Kolpin, E.T. Furlong, M.T. Meyer, E.M. Thurman, S.D. Zaugg, L.B. Barber, H.T. Buxton, Pharmaceuticals, hormones, and other organic wastewater contaminants in U.S. streams, 1999–2000: a national reconnaissance, *Environ. Sci. Technol.*, 36 (2002) 1202–1211.
- [6] M. Pan, L.M. Chu, Fate of antibiotics in soil and their uptake by edible crop, *Sci. Total Environ.*, 599–600 (2017) 500–512.
- [7] S. Foteinis, A.G.L. Borthwick, Z. Frontistis, D. Mantzavinos, E. Chatzisympson, Environmental sustainability of light-driven processes for wastewater treatment applications, *J. Cleaner Prod.*, 182 (2018) 8–15.
- [8] B. Varga, V. Somogyi, M. Meiczinger, N. Kováts, E. Domokos, Enzymatic treatment and subsequent toxicity of organic micropollutants using oxidoreductases – a review, *J. Cleaner Prod.*, 221 (2019) 306–322.
- [9] Y. Ma, L. Yang, L. Wu, P. Li, X. Qi, L. He, S. Cui, Y. Ding, Z. Zhang, Carbon nanotube supported sludge biochar as an efficient adsorbent for low concentrations of sulfamethoxazole removal, *Sci. Total Environ.*, 718 (2020) 137299, doi: 10.1016/j.scitotenv.2020.137299.
- [10] G. Jaria, V. Calisto, M.V. Gil, P. Ferreira, S.M. Santos, M. Otero, V.I. Esteves, Effects of thiol functionalization of a waste-derived activated carbon on the adsorption of sulfamethoxazole from water: kinetic, equilibrium and thermodynamic studies, *J. Mol. Liq.*, 323 (2021) 115003, doi: 10.1016/j.molliq.2020.115003.
- [11] J.C. Serna-Carrizales, V.H. Collins-Martínez, E. Flórez, C.F.A. Gomez-Duran, G. Palestino, R. Ocampo-Pérez, Adsorption of sulfamethoxazole, sulfadiazine and sulfamethazine in single and ternary systems on activated carbon. Experimental and DFT computations, *J. Mol. Liq.*, 324 (2021) 114740, doi: 10.1016/j.molliq.2020.114740.
- [12] F. Yu, Y. Li, S. Han, J. Ma, Adsorptive removal of antibiotics from aqueous solution using carbon materials, *Chemosphere*, 153 (2016) 365–385.
- [13] M.B. Ahmed, J.L. Zhou, H.H. Ngo, W. Guo, M.A.H. Johir, K. Sornalingam, Single and competitive sorption properties and mechanism of functionalized biochar for removing sulfonamide antibiotics from water, *Chem. Eng. J.*, 311 (2017) 348–358.
- [14] Y. Liu, X. Liu, G. Zhang, T. Ma, T. Du, Y. Yang, S. Lu, W. Wang, Adsorptive removal of sulfamethazine and sulfamethoxazole from aqueous solution by hexadecyl trimethyl ammonium bromide modified activated carbon, *Colloids Surf., A*, 564 (2019) 131–141.

- [15] X. Ren, C. Chen, M. Nagatsu, X. Wang, Carbon nanotubes as adsorbents in environmental pollution management: a review, *Chem. Eng. J.*, 170 (2011) 395–410.
- [16] O.G. Apul, T. Karanfil, Adsorption of synthetic organic contaminants by carbon nanotubes: a critical review, *Water Res.*, 68 (2015) 34–55.
- [17] J. Wei, W. Sun, W. Pan, X. Yu, G. Sun, H. Jiang, Comparing the effects of different oxygen-containing functional groups on sulfonamides adsorption by carbon nanotubes: experiments and theoretical calculation, *Chem. Eng. J.*, 312 (2017) 167–179.
- [18] C. Peiris, S.R. Gunatilake, T.E. Mlsna, D. Mohan, M. Vithanage, Biochar based removal of antibiotic sulfonamides and tetracyclines in aquatic environments: a critical review, *Bioresour. Technol.*, 246 (2017) 150–159.
- [19] S.Y. Lagergren, Zur theorie der sogenannten adsorption gelöster stoffe, *Kungliga Svenska Vetenskapsakademiens, Handlingar*, 24 (1898) 1–39.
- [20] Y.S. Ho, G. McKay (Fellow), Kinetic models for the sorption of dye from aqueous solution by wood, *Process Saf. Environ. Prot.*, 76 (1998) 183–191.
- [21] W.J. Weber Jr., J.C. Morris, Kinetics of adsorption on carbon from solutions, *J. Sanit. Eng. Div., Am. Soc. Civ. Eng.*, 89 (1963) 31–60.
- [22] Y. Li, M.A. Taggart, C. McKenzie, Z. Zhang, Y. Lu, S. Pap, S. Gibb, Utilizing low-cost natural waste for the removal of pharmaceuticals from water: mechanisms, isotherms and kinetics at low concentrations, *J. Cleaner Prod.*, 227 (2019) 88–97.
- [23] S. Pi, A. Li, D. Cui, Z. Su, L. Feng, F. Ma, J. Yang, Biosorption behavior and mechanism of sulfonamide antibiotics in aqueous solution on extracellular polymeric substances extracted from *Klebsiella* sp. J1, *Bioresour. Technol.*, 272 (2019) 346–350.
- [24] M.-Y. Chang, R.-S. Juang, Adsorption of tannic acid, humic acid, and dyes from water using the composite of chitosan and activated clay, *J. Colloid Interface Sci.*, 278 (2004) 18–25.
- [25] Y. Liu, Y. Peng, B. An, L. Li, Y. Liu, Effect of molecular structure on the adsorption affinity of sulfonamides onto CNTs: batch experiments and DFT calculations, *Chemosphere*, 246 (2020) 125778, doi: 10.1016/j.chemosphere.2019.125778
- [26] X. Zhang, Y. Zhang, H.H. Ngo, W. Guo, H. Wen, D. Zhang, C. Li, L. Qi, Characterization and sulfonamide antibiotics adsorption capacity of spent coffee grounds based biochar and hydrochar, *Sci. Total Environ.*, 716 (2020) 137015, doi: 10.1016/j.scitotenv.2020.137015.
- [27] S. Zhang, T. Shao, S.S.K. Bekaroglu, T. Karanfil, Adsorption of synthetic organic chemicals by carbon nanotubes: effects of background solution chemistry, *Water Res.*, 44 (2010) 2067–2074.
- [28] A. Jakubus, K. Godlewska, M. Gromelski, K. Jagiello, T. Puzyn, P. Stepnowski, M. Paszkiewicz, The possibility to use multi-walled carbon nanotubes as a sorbent for dispersive solid phase extraction of selected pharmaceuticals and their metabolites: effect of extraction condition, *Microchem. J.*, 146 (2019) 1113–1125.
- [29] W. Yang, Y. Lu, F. Zheng, X. Xue, N. Li, D. Liu, Adsorption behavior and mechanisms of norfloxacin onto porous resins and carbon nanotube, *Chem. Eng. J.*, 179 (2012) 112–118.
- [30] N.F. Nejad, E. Shams, M.K. Amini, J.C. Bennett, Ordered mesoporous carbon CMK-5 as a potential sorbent for fuel desulfurization: application to the removal of dibenzothiophene and comparison with CMK-3, *Microporous Mesoporous Mater.*, 168 (2013) 239–246.
- [31] Y. Sun, H. Li, G. Li, B. Gao, Q. Yue, X. Li, Characterization and ciprofloxacin adsorption properties of activated carbons prepared from biomass wastes by  $H_3PO_4$  activation, *Bioresour. Technol.*, 217 (2016) 239–244.
- [32] T. Santhi, S. Manonmani, T. Smitha, Removal of malachite green from aqueous solution by activated carbon prepared from the epicarp of *Ricinus communis* by adsorption, *J. Hazard. Mater.*, 179 (2010) 178–186.
- [33] X. Wei, Z. Zhang, L. Qin, J. Dai, Template-free preparation of yeast-derived three-dimensional hierarchical porous carbon for highly efficient sulfamethazine adsorption from water, *J. Taiwan Inst. Chem. Eng.*, 95 (2019) 532–540.
- [34] X. Yu, L. Zhang, M. Liang, W. Sun, pH-dependent sulfonamides adsorption by carbon nanotubes with different surface oxygen contents, *Chem. Eng. J.*, 279 (2015) 363–371.
- [35] S.W. Nam, C. Jung, H. Li, M. Yu, J.R.V. Flora, L.K. Boateng, N. Her, K.D. Zoh, Y. Yoon, Adsorption characteristics of diclofenac and sulfamethoxazole to graphene oxide in aqueous solution, *Chemosphere*, 136 (2015) 20–26.
- [36] H. Zhao, X. Liu, Z. Cao, Y. Zhan, X. Shi, Y. Yang, J. Zhou, J. Xu, Adsorption behavior and mechanism of chloramphenicols, sulfonamides, and non-antibiotic pharmaceuticals on multi-walled carbon nanotubes, *J. Hazard. Mater.*, 310 (2016) 235–245.
- [37] Y. Gao, Q. Yue, B. Gao, Y. Sun, Optimization preparation of activated carbon from *Enteromorpha prolifera* using response surface methodology and its adsorption studies of fluoroquinolone antibiotics, *Desal. Water Treat.*, 55 (2015) 624–636.
- [38] S. Deng, Q. Zhang, Y. Nie, H. Wei, B. Wang, J. Huang, G. Yu, B. Xing, Sorption mechanisms of perfluorinated compounds on carbon nanotubes, *Environ. Pollut.*, 168 (2012) 138–144.
- [39] I. Langmuir, The constitution and fundamental properties of solids and liquids, *J. Am. Chem. Soc.*, 40 (1918) 1361–1402.
- [40] H. Freundlich, Over the adsorption in solution, *J. Phys. Chem.*, 57 (1906) 385–470.
- [41] Y. Zhou, X. Liu, Y. Xiang, P. Wang, J. Zhang, F. Zhang, J. Wei, L. Luo, M. Lei, L. Tang, Modification of biochar derived from sawdust and its application in removal of tetracycline and copper from aqueous solution: adsorption mechanism and modelling, *Bioresour. Technol.*, 245 (2017) 266–273.
- [42] L. Tang, J. Yu, Y. Pang, G. Zeng, Y. Deng, J. Wang, X. Ren, S. Ye, B. Peng, H. Feng, Sustainable efficient adsorbent: alkali-acid modified magnetic biochar derived from sewage sludge for aqueous organic contaminant removal, *Chem. Eng. J.*, 336 (2018) 160–169.
- [43] L. Zheng, D. Peng, P. Meng, Promotion effects of nitrogenous and oxygenic functional groups on cadmium(II) removal by carboxylated corn stalk, *J. Cleaner Prod.*, 201 (2018) 609–623.
- [44] H. Chen, B. Gao, H. Li, Functionalization, pH, and ionic strength influenced sorption of sulfamethoxazole on graphene, *J. Environ. Chem. Eng.*, 2 (2014) 310–315.
- [45] J. Wan, H. Deng, J. Shi, L. Zhou, T. Su, Synthesized magnetic manganese ferrite nanoparticles on activated carbon for sulfamethoxazole removal, *CLEAN – Soil Air Water*, 42 (2014) 1199–1207.
- [46] Y.-K. Choi, E. Kan, Effects of pyrolysis temperature on the physicochemical properties of alfalfa-derived biochar for the adsorption of bisphenol A and sulfamethoxazole in water, *Chemosphere*, 218 (2018) 741–748.
- [47] F. Wang, W. Sun, W. Pan, N. Xu, Adsorption of sulfamethoxazole and 17 $\beta$ -estradiol by carbon nanotubes/CoFe<sub>2</sub>O<sub>4</sub> composites, *Chem. Eng. J.*, 274 (2015) 17–29.
- [48] B. Peng, L. Chen, C. Que, K. Yang, F. Deng, X. Deng, G. Shi, G. Xu, M. Wu, Adsorption of antibiotics on graphene and biochar in aqueous solutions induced by  $\pi$ - $\pi$  interactions, *Sci. Rep.*, 6 (2016) 31920, doi: 10.1038/srep31920.
- [49] A.U. Rajapaksha, M. Vithanage, M. Zhang, M. Ahmad, D. Mohan, S.X. Chang, Y.S. Ok, Pyrolysis condition affected sulfamethazine sorption by tea waste biochars, *Bioresour. Technol.*, 166 (2014) 303–308.
- [50] Q.Q. Yang, G.C. Chen, J.F. Zhang, H.L. Li, Adsorption of sulfamethazine by multiwalled carbon nanotubes: effects of aqueous solution chemistry, *RSC Adv.*, 5 (2015) 25541–25549.
- [51] Y. Liu, X. Liu, W. Dong, L. Zhang, Q. Kong, W. Wang, Efficient adsorption of sulfamethazine onto modified activated carbon: a plausible adsorption mechanism, *Sci. Rep.*, 7 (2017) 12437, doi: 10.1038/s41598-017-12805-6.
- [52] T.A.T. Aboul-Kassim, B.R.T. Simoneit, *Pollutant-Solid Phase Interactions: Mechanism, Chemistry and Modeling*, Springer-Verlag, Berlin, Heidelberg, 2001, pp. 129–132.
- [53] R.A. Dobbs, L. Wang, R. Govind, Sorption of toxic organic compounds on wastewater solids: correlation with fundamental properties, *Environ. Sci. Technol.*, 23 (1989) 1092–1097.
- [54] K. Xia, A. Bhandari, K. Das, G. Pillar, Occurrence and fate of pharmaceuticals and personal care products (PPCPs) in biosolids, *J. Environ. Qual.*, 34 (2005) 91–104.

- [55] P.Z. Sun, Y.X. Li, T. Meng, R.C. Zhang, M. Song, J. Ren, Removal of sulfonamide antibiotics and human metabolite by biochar and biochar/H<sub>2</sub>O<sub>2</sub> in synthetic urine, *Water Res.*, 147 (2018) 91–100.
- [56] H. Peng, B. Pan, M. Wu, Y. Liu, D. Zhang, B. Xing, Adsorption of ofloxacin and norfloxacin on carbon nanotubes: hydrophobicity- and structure-controlled process, *J. Hazard. Mater.*, 233–234 (2012) 89–96.
- [57] H. Nollet, M. Roels, P. Lutgen, P. Meeren, W. Verstraete, Removal of PCBs from wastewater using fly ash, *Chemosphere*, 53 (2003) 655–665.
- [58] P.W. Atkins, *Physical Chemistry*, 4th ed., Oxford University Press, London, 1990.
- [59] B. Senthil Rathi, P. Senthil Kumar, Application of adsorption process for effective removal of emerging contaminants from water and wastewater, *Environ. Pollut.*, 280 (2021) 116995, doi: 10.1016/j.envpol.2021.116995.
- [60] M. Alkan, O. Demirbaş, S. Çelikçapa, M. Doğan, Sorption of acid red 57 from aqueous solution onto sepiolite, *J. Hazard. Mater.*, 116 (2004) 135–145.
- [61] D. Zhao, G. Sheng, J. Hu, C. Chen, X. Wang, The adsorption of Pb(II) on Mg<sub>2</sub>Al layered double hydroxide, *Chem. Eng. J.*, 171 (2011) 167–174.
- [62] M. Kara, H. Yuzer, E. Sabah, M.S. Celik, Adsorption of cobalt from aqueous solutions onto sepiolite, *Water Res.*, 37 (2003) 224–232.
- [63] Y. Liu, Y.J. Liu, Biosorption isotherms, kinetics and thermodynamics, *Sep. Purif. Technol.*, 61 (2008) 229–242.